QCD Running Coupling in the Nonperturbative and Near-Perturbative Regimes

Guy F. de Téramond,[1,*] Arpon Paul,[2,†] Stanley J. Brodsky,[3,‡] Alexandre Deur,[4,§] Hans Günter Dosch,[5,‖] Tianbo Liu,[6,7,¶] and Raza Sabbir Sufian[8,9,10,**]

(HLFHS Collaboration)

[1]*Laboratorio de Física Teórica y Computacional, Universidad de Costa Rica, 11501 San José, Costa Rica*
[2]*School of Physics and Astronomy, University of Minnesota, Minneapolis, Minnesota 55455, USA*
[3]*SLAC National Accelerator Laboratory, Stanford University, Stanford, California 94309, USA*
[4]*Thomas Jefferson National Accelerator Facility, Newport News, Virginia 23606, USA*
[5]*Institut für Theoretische Physik der Universität, D-69120 Heidelberg, Germany*
[6]*Key Laboratory of Particle Physics and Particle Irradiation (MOE), Institute of Frontier and Interdisciplinary Science, Shandong University, Qingdao, Shandong 266237, China*
[7]*Southern Center for Nuclear-Science Theory (SCNT), Institute of Modern Physics, Chinese Academy of Sciences, Huizhou 516000, China*
[8]*RIKEN-BNL Research Center, Brookhaven National Laboratory, Upton, New York 11973, USA*
[9]*Physics Department, Brookhaven National Laboratory, Upton, New York 11973, USA*
[10]*Department of Physics, New Mexico State University, Las Cruces, New Mexico 88003, USA*

(Received 2 April 2024; revised 17 July 2024; accepted 20 September 2024; published 29 October 2024)

We use analytic continuation to extend the gauge-gravity duality nonperturbative description of the strong force coupling into the transition, near-perturbative, regime where perturbative effects become important. By excluding the unphysical region in coupling space from the flow of singularities in the complex plane, we derive a specific relation between the scales relevant at large and short distances; this relation is uniquely fixed by requiring maximal analyticity. The unified effective coupling model gives an accurate description of the data in the nonperturbative and the near-perturbative regions.

DOI: 10.1103/PhysRevLett.133.181901

Introduction—The running strong coupling α_s has been determined to high orders in perturbation theory at large momentum transfer: It leads to asymptotic freedom, a fundamental property of quantum chromodynamics (QCD) [1,2]. However, a purely perturbative description of α_s is inconsistent: It breaks down at the Landau pole at large distances [3]. Avoiding such unphysical singularities requires the introduction of an infrared (IR) confinement scale which effectively suppresses the long wavelength modes [4,5], or some IR regulator by adding new terms to the coupling [6,7]: Analytic couplings often lead to an IR fixed point [8]. A unified and consistent treatment of α_s in both the perturbative and nonperturbative domains should incorporate confinement dynamics, since it implies the transition from the short distance partonic degrees of freedom to the large distance hadronic degrees of freedom, the asymptotic states, where perturbative QCD is not applicable. In practice an effective description is adopted by the choice of an effective coupling subject to specific constraints.

In quantum field theory (QFT) there is some freedom in the definition of the running coupling [7,9]. Several definitions restore the coupling to the status of an observable quantity, notably the effective charge introduced by Grunberg [10,11]. It defines a QCD effective coupling $\alpha_{\rm eff}$ by the approximant of any given observable truncated to first order in the perturbative coupling α_s. This makes the effective charge definition of the QCD coupling analogous to that of QED [12]. An effective charge defined from a specific observable can be used for any process using the relations between the different effective charges [13], which guarantees the predictability of the theory. Crucially, since the leading order approximant of an

*Contact author: guy.deteramond@ucr.ac.cr
†Contact author: paul1228@umn.edu
‡Contact author: sjbth@slac.stanford.edu
§Contact author: deurpam@jlab.org
‖Contact author: h.g.dosch@gmail.com
¶Contact author: liutb@sdu.edu.cn
**Contact author: gluon2025@gmail.com

observable is scheme and gauge independent, its associated coupling is an observable as well, and therefore amenable to analytical continuation. An important advantage of $\alpha_{\rm eff}$ is that confinement forces and parton correlations are folded into its definition, thus both the IR and ultraviolet (UV) domains are incorporated.

In Ref. [14], $\alpha_{\rm eff}$ was derived in the IR domain using holographic QCD on the light-front (HLFQCD), and in Refs. [15–17] we introduced a matching procedure between HLFQCD and perturbative QCD. The procedure matches the two expressions for α_s at a single point Q_0 and yields an accurate prediction of α_s in agreement with both the IR data [18–20] and the combined world average at the Z^0 mass [21]. Yet, as we will discuss below, this prescription has its limitations. In contrast, we use analytic continuation in this Letter to extend the applicability of the nonperturbative holographic QCD description of the strong coupling into the transition, near-perturbative, regime where perturbative effects become important. Both the IR and the UV domains are incorporated into a single analytic expression providing a continuous transition between both domains for the β function and any higher derivative. In the present approach, an IR scale is required for the suppression of the unphysical Landau pole. In fact, the flow of singularities in the complex plane is responsible for the splitting of the Landau pole into two complex conjugate singularities. Furthermore, by excluding the unphysical region in coupling space, we obtain a specific relation between the mass scale underlying color confinement and the QCD scale underlying the perturbative interactions of quarks and gluons. The relation between the IR and UV scales becomes unique and leads to a single mass scale by requiring maximal analyticity in the flow of singularities. The resulting model is compared with the experimental results for the effective charge in the g_1 scheme, α_{g_1}, defined by the Bjorken sum rule [22,23], which is well measured in both the IR and UV domains.

Our approach has bearings on the analytic S-matrix bootstrap and duality concepts and tools [24–26] which arise from general principles of QFT such as symmetry, causality, unitarity, and crossing, thus, rather independently of the specific dynamics. Together with some large distance input to limit the possible solutions, this approach can lead to bounds on coupling constants [27]. Interestingly, in the pre-QCD period analytic continuation provided the connection between perturbation theory and strong interaction physics [28].

Interpolating effective coupling—In nonperturbative models, a scale is introduced to compute the hadron spectrum, whereas in a conformal gauge theory a scale, denoted by Λ for QCD, is introduced because of the necessity of perturbative renormalization. A challenge is thus to understand how these two scales are related depending on the symmetries of the underlying full theory. As general constraints required to extend the holographic strong coupling [14] beyond the IR, we demand the vanishing of the β function in the deep IR and UV to reflect the underlying conformal symmetry of QCD and the analyticity of $\alpha_{\rm eff}$ for all possible physical solutions consistent with the continuity of the physical observables.

The large N_C limit [29] underlies the holographic approach to strongly coupled QFT. In fact, the AdS/CFT duality, the correspondence between a classical gravity theory in a five-dimensional anti–de Sitter (AdS) space and a conformal field theory (CFT) in physical space-time, corresponds to the large N_C limit of a conformal theory in the UV asymptotic AdS boundary [30–32]. This should remain true if we modify the IR region of AdS space to introduce confinement. Our approach to HLFQCD is based on the embedding of Dirac's relativistic front form of dynamics [33] into AdS space. It leads to relativistic boost-invariant wave equations in physical space-time, similar to the Schrödinger equation in atomic physics [34,35]. In HLFQCD, an IR mass scale can be introduced from an emerging superconformal symmetry [36–38] by constructing a scale-deformed supercharge operator, which is a superposition of supercharges within the extended graded algebra [37]. This procedure determines uniquely the confining interaction [39–41], as well as the corresponding modification of AdS space in the IR domain [42,43], while keeping the action conformal invariant [36]; it also leads to hadronic supersymmetry between mesons, baryons, and tetraquarks [41].

To build a specific model, we thus demand that in the deep IR and UV domains the β function vanishes. In fact, it is clear from a physical perspective that, in a confining theory, quarks and gluons have a maximal wavelength, and thus all vacuum polarization corrections to the gluon self-energy must decouple: An infrared fixed point is a natural consequence of confinement [44]. Our expression for $\alpha_{\rm eff}$ incorporates the holographic results in Ref. [14], compatible with superconformal symmetry and consistent with measurements of the strong coupling in the IR [20]. In the deep UV we will recover the leading perturbative QCD logarithmic dependence. As for the analytic continuation, our model leads to the splitting of the Landau pole into two complex conjugate singularities, thus transforming the unphysical singularities in the real axis into a singularity flow in the complex Q^2 plane for the physical solutions.

We express $\alpha_{\rm eff}$ in the spacelike domain by

$$\alpha_{\rm eff}(Q^2) = \alpha_{\rm eff}(0)\exp\left[-\int_0^{Q^2}\frac{du}{4\kappa^2 + u\ln\left(\frac{u}{\Lambda^2}\right)}\right], \quad (1)$$

which satisfies the constraints described above. Here, $Q^2 = -q^2$ is the virtuality scale, κ is the IR mass scale in holographic QCD, Λ is the QCD scale governing the logarithmic evolution of the coupling in the UV, and $\alpha_{\rm eff}(0)$ is the QCD coupling's IR fixed point value. In

the g_1 scheme used here, it is fixed to π by simple kinematical constraints.

Equation (1) constrains both the deep IR and UV's behavior:

$$\alpha_{\rm eff}(Q^2) \to e^{-Q^2/4\kappa^2}, \quad \text{for } Q^2 \ll 4\kappa^2, \tag{2}$$

the Gaussian expression found in [14], and

$$\alpha_{\rm eff}(Q^2) \to \frac{1}{\ln(Q^2/\Lambda^2)}, \quad \text{for } Q^2 \gg 4\kappa^2, \tag{3}$$

the leading logarithmic Q^2 dependence. Thus, Eq. (1) provides a continuous transition between the IR and the UV perturbative domains. The β function

$$\begin{aligned}\beta(\alpha_{\rm eff}) &= Q^2 \frac{d\alpha_{\rm eff}(Q^2)}{dQ^2} \\ &= -\frac{Q^2}{4\kappa^2 + Q^2 \ln\left(\frac{Q^2}{\Lambda^2}\right)} \alpha_{\rm eff}(Q^2)\end{aligned} \tag{4}$$

has a minimum at the turning point $Q^2 = 2\kappa^2$, independent of the value of Λ, and vanishes in the deep IR and UV limits. The analytic expression (4) evolves continuously from the IR to the UV functional forms of the β function, namely from the nonperturbative expression in holographic QCD [14] to the leading perturbative expression [7]

$$\beta(\alpha_{\rm eff}) \to -\frac{Q^2}{4\kappa^2}\alpha_{\rm eff}(Q^2), \qquad Q^2 \ll 4\kappa^2, \tag{5}$$

$$\beta(\alpha_{\rm eff}) \to -\alpha_{\rm eff}^2(Q^2), \qquad Q^2 \gg 4\kappa^2. \tag{6}$$

The large N_C limit should remain valid when we extend $\alpha_{\rm eff}$ to the transition domain. This constraint implies no flavor dependence in Eq. (1) since in this limit the 't Hooft coupling $\lambda_N = g^2 N_C$, for fixed λ_N, becomes independent of the number of flavors [29]. The effective coupling $\alpha_{\rm eff}$ in (1) is thus valid in the nonperturbative and the near-perturbative domains. However, it remains an approximation in the deep, fully perturbative, UV region, since there are no quark mass thresholds in the conformal limit on which the present derivation is based.

Analytic continuation and singularity flows—General considerations of symmetry and analyticity have guided us to the expression of $\alpha_{\rm eff}$ given by Eq. (1). Analytic continuation of this expression leads us to study the flow of singularities in the complex Q^2 plane which imposes strict constraints on possible solutions. The actual flow follows from the equation

$$4\kappa^2 + Q^2 \ln\left(\frac{Q^2}{\Lambda^2}\right) = 0, \tag{7}$$

which determines the singularities of $\alpha_{\rm eff}(Q^2)$ (1) and its β function (4) in the spacelike domain $Q^2 \geq 0$. Its solutions are given by

$$Q_u^2(\kappa^2) = \Lambda^2 \exp\left[W_0\left(-\frac{4\kappa^2}{\Lambda^2}\right)\right], \tag{8}$$

and

$$Q_l^2(\kappa^2) = \Lambda^2 \exp\left[W_{-1}\left(-\frac{4\kappa^2}{\Lambda^2}\right)\right], \tag{9}$$

for fixed Λ, where u and l refer, respectively, to the solutions in the upper and lower Q^2 half-planes. $W_k(z)$, the Lambert function, is a multivalued function with a branch for each positive and negative integer value of k. It is also useful to express κ as a function of Q^2 along the locus of the solutions of (7)

$$\kappa^2(Q^2) = -\frac{1}{4}Q^2 \ln\left(\frac{Q^2}{\Lambda^2}\right), \tag{10}$$

with $Q^2 \to Q_{u,l}^2$.

In the limit $\kappa \to 0$ we find the solutions

$$Q_u^2(\kappa^2 = 0) = \Lambda^2 \quad \text{and} \quad Q_l^2(\kappa^2 = 0) = 0. \tag{11}$$

The first solution, Q_u, which corresponds to the principal branch of the Lambert function with $W_0(0) = 0$, gives the Landau singularity at $Q^2 = \Lambda^2$, and the second solution, Q_l, which corresponds to a lower branch, leads to an additional singularity at $Q^2 = 0$ since $W_{-1}(0) = -\infty$.

For small $\kappa > 0$ the distance between the two singularities, located initially in the limit $\kappa \to 0$ at $Q^2 = \Lambda^2$ and $Q^2 = 0$, starts to shrink until they meet at a point determined by the maximal value of κ in the interval $0 < Q^2 < \Lambda^2$ on the real axis, thus by the condition $d\kappa^2(Q^2)/dQ^2 = 0$, with the solution $Q^2 = \Lambda^2/e$ as shown in Fig. 1. Also from (10) we find the critical value $\kappa^2 = \Lambda^2/4e$ (see Table I), thus the two singularities merge at the critical point

$$Q_u^2\left(\kappa^2 = \frac{1}{4e}\Lambda^2\right) = \frac{1}{e}\Lambda^2 \quad \text{and} \quad Q_l^2\left(\kappa^2 = \frac{1}{4e}\Lambda^2\right) = \frac{1}{e}\Lambda^2, \tag{12}$$

since $W_0[-(1/e)] = W_{-1}[-(1/e)] = -1$. For $\kappa^2 \leq \Lambda^2/4e$ the integral in Eq. (1) is not defined since the singularities are located on the real axis where the integration is performed.

One can combine the linear Cauchy-Riemann differential equations into the second order equations $\nabla^2 {\rm Re}\,\kappa^2 = 0$ and $\nabla^2 {\rm Im}\,\kappa^2 = 0$. This implies that a maximum (minimum) of ${\rm Re}\,\kappa^2$ (${\rm Im}\,\kappa^2$) along the real Q^2 axis

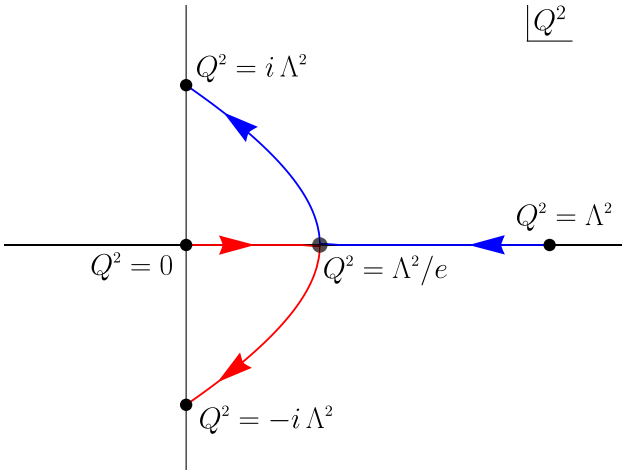

FIG. 1. Flow of singularities in the complex Q^2 plane from the solutions of (7) upon variation of κ^2 between $0 \le \kappa^2 \le (\pi/8)\Lambda^2$ for fixed Λ; the flow paths of Q_u and Q_l [Eqs. (8) and (9)] are marked blue and red, respectively. The critical value $\kappa^2 = \Lambda^2/4e$ corresponds to the bifurcation point at $Q^2 = \Lambda^2/e$. The effective coupling (1) is not defined for $\kappa^2 < \Lambda^2/4e$. For values of $\kappa^2 > \Lambda^2/4e$, the double pole at the critical bifurcation point is split into two complex conjugate singularities, and the coupling (1) can be computed for any value of Q^2. The upper limit for κ leads to the relation $\Lambda^2 = (8/\pi)\kappa^2$ between the confinement and QCD scales κ and Λ. See also Table I.

corresponds to a minimum (maximum) of $\mathrm{Re}\,\kappa^2$ ($\mathrm{Im}\,\kappa^2$) along the imaginary direction, thus to a saddle point located at $Q_u^2 = Q_d^2 = \Lambda^2/e$ for $\kappa^2 = \Lambda^2/4e$, as shown in Fig. 2 (left) for $\mathrm{Re}\,\kappa^2$. We also verify in Fig. 2 (right), by taking the intersection of $\mathrm{Im}\,\kappa^2$ with the plane $\mathrm{Im}\,\kappa^2 = 0$, that, as expected, κ^2 is real on the singularity flow. The gradient vectors $\vec{\nabla}\mathrm{Re}\,\kappa^2$ and $\vec{\nabla}\mathrm{Im}\,\kappa^2$ are mutually orthogonal, $\vec{\nabla}\mathrm{Re}\,\kappa^2 \cdot \vec{\nabla}\mathrm{Im}\,\kappa^2 = 0$, and normal, respectively, to the two curves $\mathrm{Re}\,\kappa^2 = \text{constant}$ and $\mathrm{Im}\,\kappa^2 = \text{constant}$. For both $\mathrm{Re}\,\kappa^2$ and $\mathrm{Im}\,\kappa^2$, there is an intersection between two level curves at the saddle point $Q^2 = \Lambda^2/e$, as depicted in the bottom projection planes in Fig. 2. The singularity flow for real κ^2 (i.e., at $\mathrm{Im}\,\kappa^2 = 0$) follows the vector $\vec{\nabla}\mathrm{Re}\,\kappa^2$ [Fig. 2 (left)] which, because of the orthogonality of the gradient vectors $\vec{\nabla}\mathrm{Re}\,\kappa^2$ and $\vec{\nabla}\mathrm{Im}\,\kappa^2$, should follow the level curve for $\mathrm{Im}\,\kappa^2$. This is verified in the projection plane in Fig. 2 (right) for the level curve which intersects the saddle point. Hence, the singularity at the critical point $Q^2 = \Lambda^2/e$ in the real axis is a bifurcation point into two complex conjugate singularities which flow into the lower and upper half-planes of the complex plane. The bifurcation point thus represents the critical value of the IR scale κ^2 above which the coupling (1) and its β function (4)—or any higher derivative—can be computed for any value of $Q^2 \ge 0$.

TABLE I. Values for the solution of the flow equation (7), Eqs. (8) and (9), for the specific points marked with black circles in Fig. 1, and the corresponding values of κ^2 from Eq. (10).

κ^2	Q_u^2	Q_l^2
0	Λ^2	0
$\Lambda^2/4e$	Λ^2/e	Λ^2/e
$\pi\Lambda^2/8$	$i\Lambda^2$	$-i\Lambda^2$

By further increasing κ we find from (10) that the complex conjugate singularities reach the imaginary axis at the points

$$Q_u^2\left(\kappa^2 = \frac{\pi}{8}\Lambda^2\right) = i\Lambda^2 \quad \text{and} \quad Q_l^2\left(\kappa^2 = \frac{\pi}{8}\Lambda^2\right) = -i\Lambda^2, \tag{13}$$

as follows from $W_0[-(\pi/2)] = i(\pi/2)$ and $W_1[-(\pi/2)] = -i(\pi/2)$. Also from (10) we find

$$\kappa^2 = \frac{\pi}{8}\Lambda^2 \tag{14}$$

for the maximal separation of the two singularities along the imaginary axis (see Table I).

Although related by analytic continuation, the spacelike and timelike domains describe physically different processes on different domains: The singularity flow from the complex plane $Q^2 > 0$ into the timelike domain $Q^2 < 0$ in Fig. 1 is not possible. Equation (14) represents an upper bound for the value of the confinement scale κ for a given value of Λ. The limit of maximal analyticity of the effective coupling, namely the largest possible domain in the Q^2-spacelike complex plane, leads to a unique relation between the confinement scale κ and the QCD scale Λ: It implies that the effective coupling (1) is a holomorphic function in the full $Q^2 > 0$ complex plane, except at its border $Q^2 = 0$. This is compatible with general principles of QFT which require that spacelike observables are analytic functions in the Q^2-Euclidean complex plane.

Comparison with experiment—Imposing maximal analyticity also means that the effective coupling has no free parameters once the scale κ is fixed by an observable quantity, for example by the ρ mass. Furthermore, since κ is a physical quantity, it follows that Λ, in the present nonperturbative approach, is also an observable quantity: The effective coupling (1) is thus promoted from an effective interpolation formula to an effective charge, namely to the status of an observable quantity [10,11]. As mentioned above, in the limit of massless quarks there is no flavor dependence of the coupling. As an approximation to this limit we take the effective number of flavors to

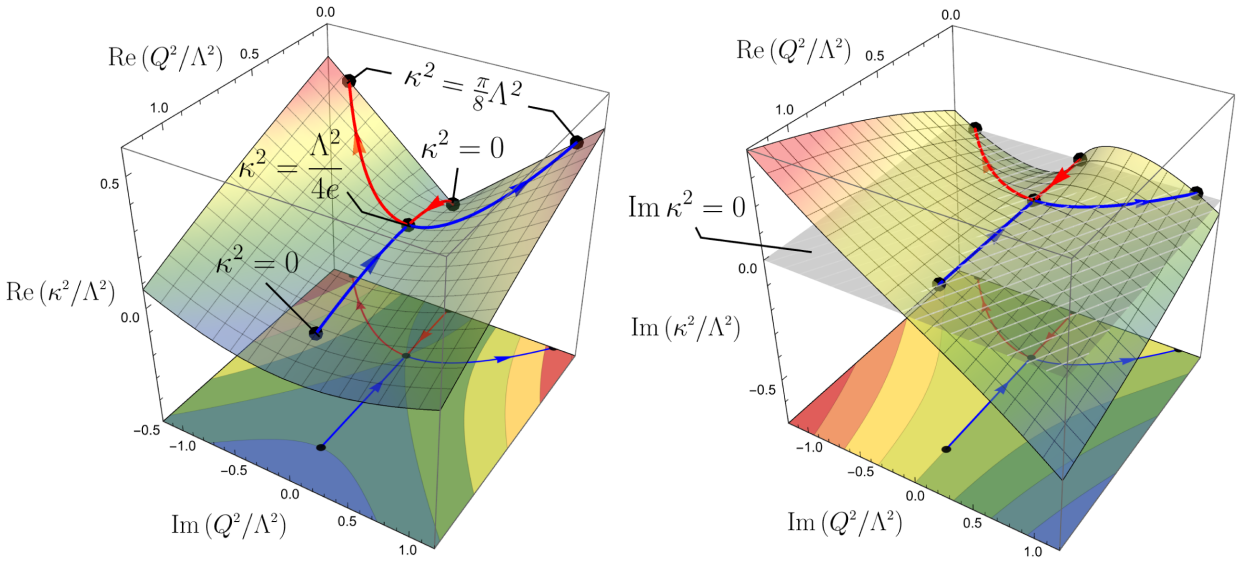

FIG. 2. Singularity flow for the real and imaginary components of κ^2 from Eq. (7). The bifurcation point of the flow in the Q^2 plane is a saddle point for $\mathrm{Re}\,\kappa^2$ (left). The intersection of the surface $\mathrm{Im}\,\kappa^2$ with the plane $\mathrm{Im}\,\kappa^2 = 0$, shown in shaded gray, illustrates that κ^2 is real along the flow (right).

$n_f = 3$. From the value $\Lambda_{g1}^{(n_f=3)} = 0.92 \pm 0.05$ GeV in the g_1 scheme [16], one obtains the value $\kappa = 0.58 \pm 0.03$ GeV in the maximal analyticity limit. It is compatible with $\kappa = 0.534 \pm 0.025$ GeV from the light vector meson spectrum in HLFQCD [45] and $\kappa = 0.523 \pm 0.024$ GeV from the light meson and baryon spectroscopy including all radial and orbital excitations [46].

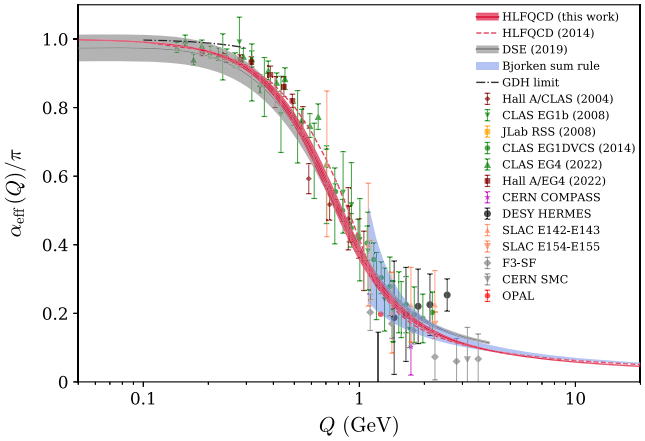

FIG. 3. Comparison of the effective strong coupling prediction from Eq. (1) with α_{g1} extracted from the available data in Refs. [47–72] and [20]. The red band corresponds to $\kappa = 0.534 \pm 0.025$ GeV and maximal analyticity (14). Here, α_{eff} is computed in the g_1 scheme, which imposes $\alpha_{\mathrm{eff}}(0) = \pi$. The dashed red curve corresponds to the point-matching procedure from Ref. [14] for $\kappa = 0.534$ GeV. Similar behavior has been obtained from Dyson-Schwinger and lattice computations in Refs. [73,74], gray band. The blue band corresponds to the perturbative 4-loop QCD prediction in the g_1 scheme [20].

We compare in Fig. 3 the predictions from Eq. (1), with available data, including the most recent measurements from Ref. [20]. The data from the Bjorken sum, listed by experiments, are from CERN [47–52], DESY [53–55], JLab [56–59] and [20], and SLAC [60–69]. The data without using the Bjorken sum are from CCFR (F3-SF) [70,71] and OPAL [72]. We use the value of $\kappa = 0.534 \pm 0.025$ GeV from [45] and the maximal quenching relation (14). The model describes accurately the experimental results in the nonperturbative and transition domains, consistent with a single scale governing the confinement dynamics of QCD.

Conclusion and outlook—The results presented here provide a new framework for extending the gauge-gravity results for the effective coupling [14] into the transition regime between a strongly coupled and an asymptotically free theory. The procedure, based on analytic continuation, is compatible with the underlying conformal symmetry properties of QCD and its large N_C constraints and incorporates the structural elements one can expect from the full theory. Instead of matching the IR and UV expressions at a given point [15–17], we introduce a single holomorphic expression, namely infinitely differentiable at any point, thus amenable to the complex analysis central to our study. The study of the possible solutions of the strong coupling determines the flow of singularities in the complex Q^2 plane leading to the splitting of the Landau pole into two complex singularities, and to a unique relation between the nonperturbative and perturbative scales which emerges in the limit of maximal analyticity. Our work identifies the hadron mass scale κ, which underlies QCD dynamics and spectroscopy in holographic light-front QCD, as the key parameter which determines the evolution

of the effective strong coupling. Moreover, it gives rise to an accurate description of the available data in the nonperturbative and the perturbative transition region.

The extension of the present results to the full perturbative domain requires a careful study of the dynamical consequences of the opening of channels at higher virtuality, since it is not possible to establish a one-to-one mapping between the iterative loop QCD results in perturbation theory with our nonperturbative approach. In the framework of the model developed here, this may be achieved by allowing for the Q^2 dependence of the confinement scale κ. Such a scale dependence is also required to describe the spectroscopy of heavy quark systems in holographic QCD [42,75,76]. The framework introduced in this Letter also naturally lends itself to the analytic continuation of our results to the entire complex plane including the timelike domain $Q^2 < 0$ [77]. These subjects are under consideration.

Acknowledgments—This work is supported in part by the Department of Energy Contract No. DE-AC02-76SF00515. It is also supported in part by the U.S. Department of Energy, Office of Science, Office of Nuclear Physics under Contract No. DE-AC05-06OR23177. T. L. is supported by the National Natural Science Foundation of China under Grants No. 12175117 and No. 12321005 and Shandong Province Natural Science Foundation Grant No. ZFJH202303. R. S. S. is supported by the Special Postdoctoral Researchers Program of RIKEN, Laboratory Directed Research and Development (LDRD No. 23-051) of Brookhaven National Laboratory and RIKEN-BNL Research Center.

[1] D. J. Gross and F. Wilczek, Ultraviolet behavior of non-Abelian gauge theories, Phys. Rev. Lett. **30**, 1343 (1973).
[2] H. D. Politzer, Reliable perturbative results for strong interactions?, Phys. Rev. Lett. **30**, 1346 (1973).
[3] L. D. Landau, A. A. Abrikosov, and I. M. Khalatnikov, The removal of infinities in quantum electrodynamics, Dokl. Akad. Nauk SSSR **95**, 607 (1954).
[4] V. N. Gribov, Quantization of non-Abelian gauge theories, Nucl. Phys. **B139**, 1 (1978).
[5] J. M. Cornwall, Dynamical mass generation in continuum QCD, Phys. Rev. D **26**, 1453 (1982).
[6] D. V. Shirkov and I. L. Solovtsov, Analytic QCD running coupling with finite IR behavior and universal $\alpha_s(0)$ value, arXiv:hep-ph/9604363.
[7] A. Deur, S. J. Brodsky, and G. F. de Téramond, The QCD running coupling, Prog. Part. Nucl. Phys. **90**, 1 (2016).
[8] C. Ayala and G. Cvetic, Mathematica and Fortran programs for various analytic QCD couplings, J. Phys. Conf. Ser. **608**, 012064 (2015).
[9] A. Deur, S. J. Brodsky, and C. D. Roberts, QCD running couplings and effective charges, Prog. Part. Nucl. Phys. **134**, 104081 (2024).
[10] G. Grunberg, Renormalization group improved perturbative QCD, Phys. Lett. **95B**, 70 (1980); **110B**, 501(E) (1982).
[11] G. Grunberg, Renormalization-scheme-invariant QCD and QED: The method of effective charges, Phys. Rev. D **29**, 2315 (1984).
[12] M. Gell-Mann and F. E. Low, Quantum electrodynamics at small distances, Phys. Rev. **95**, 1300 (1954).
[13] S. J. Brodsky and H. J. Lu, Commensurate scale relations in quantum chromodynamics, Phys. Rev. D **51**, 3652 (1995).
[14] S. J. Brodsky, G. F. de Téramond, and A. Deur, Nonperturbative QCD coupling and its β-function from light-front holography, Phys. Rev. D **81**, 096010 (2010).
[15] A. Deur, S. J. Brodsky, and G. F. de Téramond, Connecting the hadron mass scale to the fundamental mass scale of quantum chromodynamics, Phys. Lett. B **750**, 528 (2015).
[16] A. Deur, S. J. Brodsky, and G. F. de Téramond, On the interface between perturbative and nonperturbative QCD, Phys. Lett. B **757**, 275 (2016).
[17] A. Deur, S. J. Brodsky, and G. F. de Téramond, Determination of $\Lambda_{\overline{\rm MS}}$ at five loops from holographic QCD, J. Phys. G **44**, 105005 (2017).
[18] A. Deur, V. Burkert, J.-P. Chen, and W. Korsch, Experimental determination of the effective strong coupling constant, Phys. Lett. B **650**, 244 (2007).
[19] A. Deur, V. Burkert, J. P. Chen, and W. Korsch, Determination of the effective strong coupling constant $\alpha_{s,g_1}(Q^2)$ from CLAS spin structure function data, Phys. Lett. B **665**, 349 (2008).
[20] A. Deur, V. Burkert, J. P. Chen, and W. Korsch, Experimental determination of the QCD effective charge $\alpha_{g_1}(Q)$, Particles **5**, 171 (2022).
[21] R. L. Workman *et al.* (Particle Data Group), Review of particle physics, Prog. Theor. Exp. Phys. **2022**, 083C01 (2022).
[22] J. D. Bjorken, Applications of the chiral $U(6) \otimes U(6)$ algebra of current densities, Phys. Rev. **148**, 1467 (1966).
[23] J. D. Bjorken, Inelastic scattering of polarized leptons from polarized nucleons, Phys. Rev. D **1**, 1376 (1970).
[24] G. F. Chew and S. C. Frautschi, Principle of equivalence for all strongly interacting particles within the *S*-matrix framework, Phys. Rev. Lett. **7**, 394 (1961).
[25] R. J. Eden, P. V. Landshoff, D. I. Olive, and J. C. Polkinghorne, *The Analytic S-Matrix* (Cambridge University Press, Cambridge, England, 1966).
[26] G. Veneziano, Construction of a crossing-symmetric, Regge-behaved amplitude for linearly rising trajectories, Nuovo Cimento A **57**, 190 (1968).
[27] S. Mizera, Physics of the analytic S-matrix, Phys. Rep. **1047**, 1 (2024).
[28] S. Mandelstam, Analytic properties of transition amplitudes in perturbation theory, Phys. Rev. **115**, 1741 (1959).
[29] G. 't Hooft, A planar diagram theory for strong interactions, Nucl. Phys. **B72**, 461 (1974).
[30] J. M. Maldacena, The large *N* limit of superconformal field theories and supergravity, Adv. Theor. Math. Phys. **2**, 231 (1998).
[31] S. S. Gubser, I. R. Klebanov, and A. M. Polyakov, Gauge theory correlators from noncritical string theory, Phys. Lett. B **428**, 105 (1998).

[32] E. Witten, Anti-de Sitter space and holography, Adv. Theor. Math. Phys. **2**, 253 (1998).

[33] P. A. M. Dirac, Forms of relativistic dynamics, Rev. Mod. Phys. **21**, 392 (1949).

[34] G. F. de Téramond and S. J. Brodsky, Light-front holography: A first approximation to QCD, Phys. Rev. Lett. **102**, 081601 (2009).

[35] S. J. Brodsky, G. F. de Téramond, H. G. Dosch, and J. Erlich, Light-front holographic QCD and emerging confinement, Phys. Rep. **584**, 1 (2015).

[36] V. de Alfaro, S. Fubini, and G. Furlan, Conformal invariance in quantum mechanics, Nuovo Cimento A **34**, 569 (1976).

[37] S. Fubini and E. Rabinovici, Superconformal quantum mechanics, Nucl. Phys. **B245**, 17 (1984).

[38] V. P. Akulov and A. I. Pashnev, Quantum superconformal model in (1,2) space, Theor. Math. Phys. **56**, 862 (1983).

[39] S. J. Brodsky, G. F. de Téramond, and H. G. Dosch, Threefold complementary approach to holographic QCD, Phys. Lett. B **729**, 3 (2014).

[40] G. F. de Téramond, H. G. Dosch, and S. J. Brodsky, Baryon spectrum from superconformal quantum mechanics and its light-front holographic embedding, Phys. Rev. D **91**, 045040 (2015).

[41] H. G. Dosch, G. F. de Téramond, and S. J. Brodsky, Superconformal baryon-meson symmetry and light-front holographic QCD, Phys. Rev. D **91**, 085016 (2015).

[42] H. G. Dosch, G. F. de Téramond, and S. J. Brodsky, Supersymmetry across the light and heavy-light hadronic spectrum II, Phys. Rev. D **95**, 034016 (2017).

[43] G. F. de Téramond and S. J. Brodsky, Color symmetry and confinement as an underlying superconformal structure in holographic QCD, Int. J. Mod. Phys. A **39**, 2441007 (2024).

[44] S. J. Brodsky and G. F. de Téramond, Light-front dynamics and AdS/QCD correspondence: The pion form factor in the space- and time-like regions, Phys. Rev. D **77**, 056007 (2008).

[45] R. S. Sufian, T. Liu, G. F. de Téramond, H. G. Dosch, S. J. Brodsky, A. Deur, M. T. Islam, and B.-Q. Ma, Nonperturbative strange-quark sea from lattice QCD, light-front holography, and meson-baryon fluctuation models, Phys. Rev. D **98**, 114004 (2018).

[46] S. J. Brodsky, G. F. de Téramond, H. G. Dosch, and C. Lorcé, Universal effective hadron dynamics from superconformal algebra, Phys. Lett. B **759**, 171 (2016).

[47] B. Adeva *et al.* (Spin Muon Collaboration), Measurement of the spin-dependent structure function $g_1(x)$ of the deuteron, Phys. Lett. B **302**, 533 (1993).

[48] D. Adams *et al.* (Spin Muon (SMC) Collaboration), Measurement of the spin-dependent structure function $g_1(x)$ of the proton, Phys. Lett. B **329**, 399 (1994); **339**, 332(E) (1994).

[49] B. Adeva *et al.* (Spin Muon (SMC) Collaboration), The spin-dependent structure function $g_1(x)$ of the proton from polarized deep-inelastic muon scattering, Phys. Lett. B **412**, 414 (1997).

[50] D. Adams *et al.* (Spin Muon Collaboration), A new measurement of the spin dependent structure function $g_1(x)$ of the deuteron, Phys. Lett. B **357**, 248 (1995).

[51] D. Adams *et al.* (Spin Muon (SMC) Collaboration), Spin structure of the proton from polarized inclusive deep-inelastic muon-proton scattering, Phys. Rev. D **56**, 5330 (1997).

[52] M. G. Alekseev *et al.* (COMPASS Collaboration), The spin-dependent structure function of the proton g_1^p and a test of the Bjorken sum rule, Phys. Lett. B **690**, 466 (2010).

[53] K. Ackerstaff *et al.* (HERMES Collaboration), Determination of the deep inelastic contribution to the generalized Gerasimov-Drell-Hearn integral for the proton and neutron, Phys. Lett. B **444**, 531 (1998).

[54] A. Airapetian *et al.* (HERMES Collaboration), The Q^2-dependence of the generalized Gerasimov-Drell-Hearn integral for the proton, Phys. Lett. B **494**, 1 (2000).

[55] A. Airapetian *et al.* (HERMES Collaboration), The Q^2 dependence of the generalized Gerasimov-Drell-Hearn integral for the deuteron, proton and neutron, Eur. Phys. J. C **26**, 527 (2003).

[56] A. Deur *et al.*, Experimental determination of the evolution of the Bjorken integral at low Q^2, Phys. Rev. Lett. **93**, 212001 (2004).

[57] A. Deur *et al.*, Experimental study of isovector spin sum rules, Phys. Rev. D **78**, 032001 (2008).

[58] A. Deur, Y. Prok, V. Burkert, D. Crabb, F. X. Girod, K. A. Griffioen, N. Guler, S. E. Kuhn, and N. Kvaltine, High precision determination of the Q^2 evolution of the Bjorken Sum, Phys. Rev. D **90**, 012009 (2014).

[59] A. Deur *et al.*, Experimental study of the behavior of the Bjorken sum at very low Q^2, Phys. Lett. B **825**, 136878 (2022).

[60] K. Abe *et al.* (E143 Collaboration), Precision measurement of the proton spin structure function g_1^p, Phys. Rev. Lett. **74**, 346 (1995).

[61] K. Abe *et al.* (E143 Collaboration), Precision measurement of the deuteron spin structure function g_1^d, Phys. Rev. Lett. **75**, 25 (1995).

[62] P. L. Anthony *et al.* (E142 Collaboration), Deep inelastic scattering of polarized electrons by polarized ^{3}He and the study of the neutron spin structure, Phys. Rev. D **54**, 6620 (1996).

[63] K. Abe *et al.* (E143 Collaboration), Measurements of the Q^2 dependence of the proton and deuteron spin structure functions g_1^p and g_1^d, Phys. Lett. B **364**, 61 (1995).

[64] K. Abe *et al.* (E143 Collaboration), Measurements of the proton and deuteron spin structure function g_1 in the resonance region, Phys. Rev. Lett. **78**, 815 (1997).

[65] K. Abe *et al.* (E154 Collaboration), Precision determination of the neutron spin structure function g_1^n, Phys. Rev. Lett. **79**, 26 (1997).

[66] K. Abe *et al.* (E154 Collaboration), Next-to-leading order QCD analysis of polarized deep inelastic scattering data, Phys. Lett. B **405**, 180 (1997).

[67] K. Abe *et al.* (E143 Collaboration), Measurements of the proton and deuteron spin structure functions g_1 and g_2, Phys. Rev. D **58**, 112003 (1998).

[68] P. L. Anthony *et al.* (E155 Collaboration), Measurement of the deuteron spin structure function $g_1^d(x)$ for $1-(\mathrm{GeV}/c)^2 < Q^2 < 40-(\mathrm{GeV}/c)^2$, Phys. Lett. B **463**, 339 (1999).

[69] P. L. Anthony *et al.* (E155 Collaboration), Measurements of the Q^2 dependence of the proton and neutron spin structure functions g_1^p and g_1^n, Phys. Lett. B **493**, 19 (2000).

[70] J. H. Kim *et al.*, A measurement of $\alpha_s(Q^2)$ from the Gross-Llewellyn Smith sum rule, Phys. Rev. Lett. **81**, 3595 (1998).

[71] J. Chyla and A. L. Kataev, Next-to-next-to-leading order QCD analysis of the Gross-Llewellyn Smith sum rule and the higher twist effects, Phys. Lett. B **297**, 385 (1992).

[72] S. J. Brodsky, S. Menke, C. Merino, and J. Rathsman, On the behavior of the effective QCD coupling $\alpha_\tau(s)$ at low scales, Phys. Rev. D **67**, 055008 (2003).

[73] D. Binosi, C. Mezrag, J. Papavassiliou, C. D. Roberts, and J. Rodriguez-Quintero, Process-independent strong running coupling, Phys. Rev. D **96**, 054026 (2017).

[74] Z.-F. Cui, J.-L. Zhang, D. Binosi, F. de Soto, C. Mezrag, J. Papavassiliou, C. D. Roberts, J. Rodríguez-Quintero, J. Segovia, and S. Zafeiropoulos, Effective charge from lattice QCD, Chin. Phys. C **44**, 083102 (2020).

[75] T. Gutsche, V. E. Lyubovitskij, I. Schmidt, and A. Vega, Chiral symmetry breaking and meson wave functions in soft-wall AdS/QCD, Phys. Rev. D **87**, 056001 (2013).

[76] M. Nielsen, S. J. Brodsky, G. F. de Téramond, H. G. Dosch, F. S. Navarra, and L. Zou, Supersymmetry in the double-heavy hadronic spectrum, Phys. Rev. D **98**, 034002 (2018).

[77] J. Horak, J. M. Pawlowski, J. Turnwald, J. M. Urban, N. Wink, and S. Zafeiropoulos, Nonperturbative strong coupling at timelike momenta, Phys. Rev. D **107**, 076019 (2023).